Int J Clin Exp Pathol 2015;8(9):10555-10564
www.ijcep.com /ISSN:1936-2625/IJCEP0013305

Original Article

Bone marrow mesenchymal stromal cells with CD47 high expression via the signal transducer and activators of transcription signaling pathway preventing myocardial fibrosis

Wei Deng, Qing-Wei Chen, Xing-Sheng Li, Zhong-Ming Yuan, Gui-Qiong Li, Da-Zhi Ke, Li Wang, Zhi-Qing Wu, Shi-Lan Luo

Department of Gerontology, The No. 2 Hospital Affiliated to Chongqing Medical University, Chongqing 400010, China

Received July 23, 2015; Accepted August 26, 2015; Epub September 1, 2015; Published September 15, 2015

Abstract: This study was initiated to investigate the efficacy of myocardial fibrosis intervention via signal transducer and activators of transcription (STAT) signaling using bone marrow (BM) mesenchymal stromal cells (MSC) in which being over-expressed with the aid of bispecific antibody (BiAb) and ultrasound-mediated microbubbles (MB). BiAb was prepared and combined with isolated MSC with CD47 overexpression from male mice and trans-fused into female mice with isoproterenol-induced myocardial fibrosis via the tail vein, followed by MB. This study included five groups. Five weeks after treatment, expression levels of the sex-determining region of Y-chromosome (SRY), matrix metalloproteinases (MMP)-9, tissue inhibitor of metalloproteinase (TIMP)-1 and vascular endothelial growth factor (VEGF) in myocardium were detected by fluorescent quantitative real-time polymerase chain reaction (qRT-PCR). The protein expression of signal transducer and activators of transcription (STAT) 1 and STAT 3 was detected by Western blot. Results: The highest homing number of MSC was in the CD47 + MSC + BiAb + MB group, second highest in the CD47 + MSC + BiAb group, and lowest in MSC alone. Compared with the Control group, CD47 + MSC + BiAb + MB, CD47 + MSC + BiAb, CD47 + MSC and MSC groups had decreased levels of MMP-9, TIMP-1, STAT 1 and collagen deposition, and increased levels of STAT 3. Up regulated STAT 3 and down regulated TIMP-1 were significantly different in CD47 + MSC + BiAb + MB compared with CD47 + MSC or CD47 + MSC + BiAb. Conclusion: CD47 can enhance the homing rate and repairing efficacy of MSC. MSC can improve MMP-TIMP expression in injured myocardium and interfere with myocardial fibrosis after homing, a mechanism that may be related to the STAT-mediated signaling pathway.

Keywords: Myocardial fibrosis, mesenchymal stromal cells, CD47, signal transducer and activators of transcription

Introduction

Myocardial fibrosis is a pathological feature at the end stage of some cardiovascular diseases and characterized by the proliferation of cardiac fibroblasts in the myocardial interstitium, the transformation of these fibroblasts into myofibroblasts and the excessive deposition of extracellular matrix (ECM) [1]. Bone marrow (BM)-derived mesenchymal stem cells (MSCs) transplantation has been used in drug intervention, interventional therapy and surgery for the treatment of ischemic heart disease because they have the ability to differentiate in to cardiomyocyte or cardiomyocyte-like cells and repair myocardial infarction. However, numerous animal experiments and clinical trials have shown that the repairing efficacy of BMSCs transplantation is often limited by the migratory number and colonization amount of targeted stem cells [2].

Recent studies have demonstrated that more than 60% implanted stem cells are retentated by lung, liver, spleen and other non-target organ rejection in transplanted host body, and the number of valid stem cell homing to the damaged target tissue rarely. This directly affects

Table 1. The mRNA expression of MMP-9, TIMP-1 and VEGF in myocardium of the five groups of rat by qRT-PCR

Gene	Control	MSC	CD47 + MSC	CD47 + MSC + BiAb	CD47 + MSC + BiAb + MB
MMP-9/β-actin	4.31±0.3	3.16±0.25[a]	2.71±0.34[b]	2.93±0.24[c]	1.83±0.16[d]
TIMP-1/β-actin	0.92±0.06	0.78±0.03[a]	0.65±0.03[b]	0.62±0.02[c]	0.41±0.08[d]
STAT 1	1.03±0.08	0.83±0.04[a]	0.67±0.04[b]	0.66±0.12[c]	0.43±0.02[d]
VEGF	0.35±0.05	0.54±0.03[a]	0.85±0.03[b]	0.82±0.04[c]	1.01±0.05[d]
STAT 3	0.3±0.03	0.83±0.04[e]	0.8±0.03	0.79±0.03	1±0.02[d]

Note: a standing for Control Vs MSC; b standing for Control Vs CD + 47 + MSC; c standing for CD47 + MSC + BiAb Vs Control; d standing for CD47 + MSC + BiAb + MB Vs control; e standing for MSC Vs CD47 + MSC + BiAb.

the effectiveness of stem cells to repair [3]. The most commonly used three stem cell transplantation approaches have certain limitations: I Intracoronary transplanted restricted to coronary condition and special equipment; II Transendocardial and epicardial injection require sophisticated equipment and precise positioning; III Intravenous transplanted safe, easy to operate, but poor targeting and low efficiency. Therefore, developing a method, by which stem cell transplantation not only from the vein, but also increased its survival rate, to ameliorate the therapeutic effect of cell cardiomyoplasty is extremely important [4-6].

CD47 is involved in a range of cellular processes, including apoptosis, proliferation, adhesion, and migration [7-10]. Furthermore, it plays a key role in immune and angiogenic responses. Considerable researches have shown that CD47 has the ability to evade the immune cells phagocytosis as an exempted mark of cell death. Monocytes-macrophages removed the damaged cells in the bloodstream and exogenous foreign body by primarily monitoring cell surface CD47. CD47 molecules can be recognized by receptor signal-regulated protein α on the cell surface of macrophages, which can protect cells carry CD47 against the phagocytosis. It has been suggested that genetic modification of BMSC with CD47 can enhance the stem cell therapies. However, the molecular mechanism underling this was unclear.

In order to promote the homing of MSC and understand its repairing mechanism, we combined bispecific antibody (BiAb) and ultrasound-mediated microbubbles (MB) to guide MSC with CD47 high expression to improve the homing number of MSC and evaluate the therapeutic efficacy of this treatment on myocardial fibrosis.

Materials and methods

Animals

One-hundren male Sprague-Dawley (SD) rats (Shanghai Slac Laboratory Animal Co. Ltd., China) were used in this study. The animal protocol was in compliance with the Guide for the Care and Use of Laboratory Animals published by the US National Institute of Health (NIH Publication No. 85-23, revised 1996) and was approved by the Experimental Animal Care Committee of Chongqing Medical University, Chongqing, China.

Preparation of BMSCs

Flow cytometry was used to detect the markers of BMSCs (P3) that included the cells positive for CD29, CD44, and CD90 and negative for CD34 and CD45. Adipogenic induction medium and osteogenic induction medium were then added to induce differentiation into adipocytes or osteoblasts, respectively.

Preparation of BiAb

Rabbit anti-rat CD29 (Bioss, Beijing, China) was dissolved in Traut's reagent (Pierce, Rockford, IL, USA) for 1 h according to the chemical cross-linking method. Anti-myosin light chain antibody (AMLCA) (Abcam, Cambridge, UK) was dissolved in Sulpho-SMCC reagent (Pierce) for 1 h. Both monoclonal antibodies were mixed immediately in equimolar proportions and kept overnight at 4°C. The BiAb was identified using non-reductive sodium dodecyl sulfate (SDS)-polyacrylamide gel electrophoresis (PAGE).

Management of ultrasound-mediated MB

MB were awarded the National Invention Patent of China in 2005 and have been widely applied

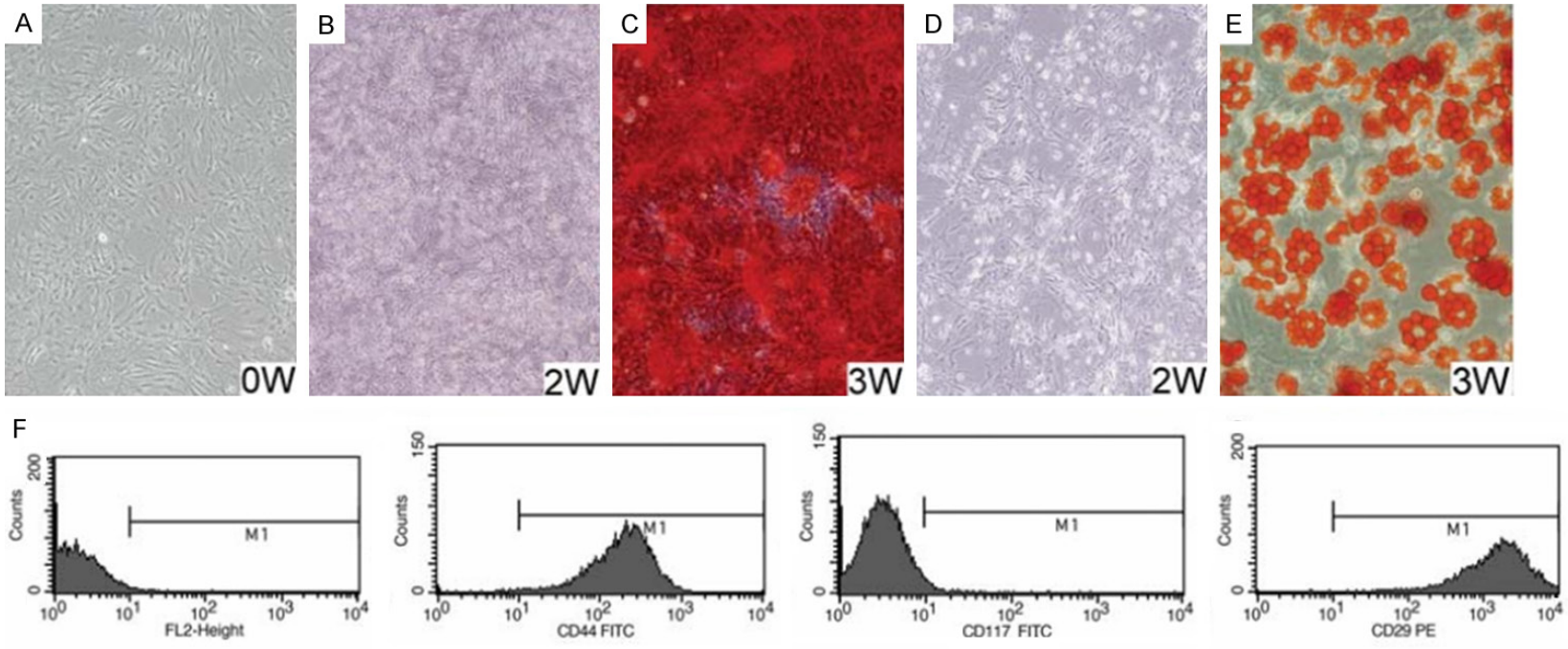

Figure 1. MSC identification using morphologic classification, functional indexes and cellular phenotyping.

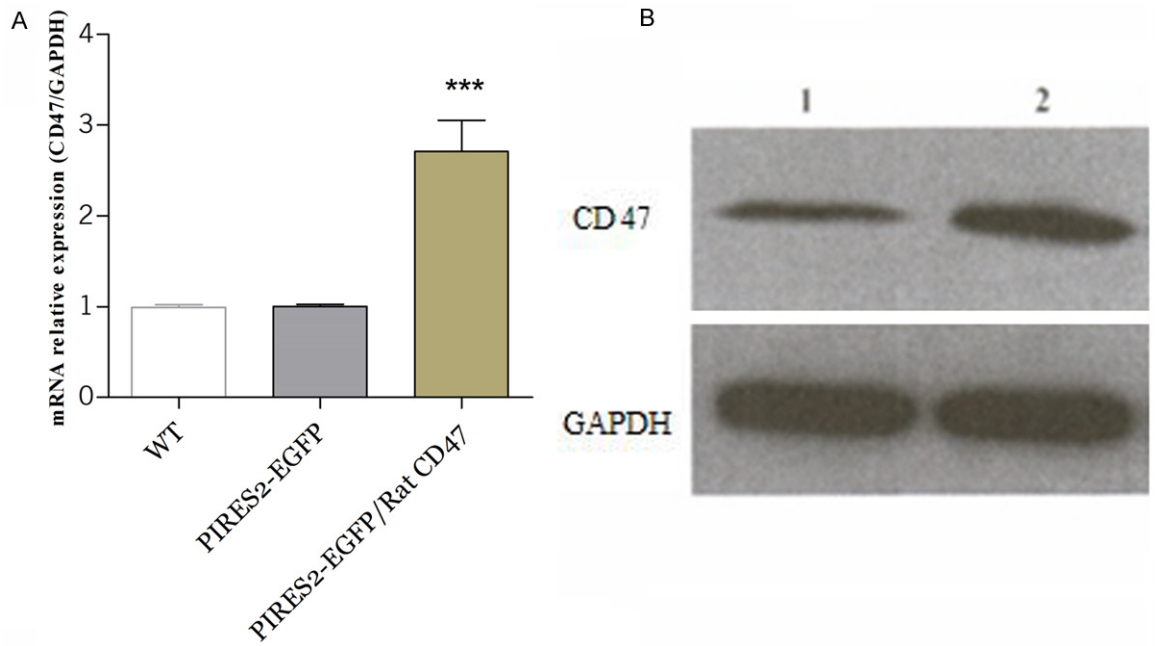

Figure 2. The expression of CD47 in BMS after transfection A: mRNA expression, B: Protein expression.

in experimental studies. The ultrasound treatment meter Type UGT 1025 (10-12) was developed by the Institute of Ultrasound Imaging, Chongqing Medical University. The concentration of MB used was approximately 8.5×10^8 bubbles/mL. Ultrasound irradiation was performed at a frequency of 1 MHz and an intensity of 1.5 W/cm^2 for 1 min.

Construction of CD47 over-erpression vector and cell transfection

The rat CD47 cDNA sequence was derived from NCBI gene bank. Recognition sites sequence of Xho1 and EcoR I restriction enzymes were added to 5' ends of reverse and forward primers to introduce Xho I site at the 5' and EcoR I site (Italics

and bold) at the 3' end of the PCR products. We included the sequence between Xho I site and SnaBI site (underlined) in the 5' site of the CD47-fwd primer after the XhoI recognition site sequence. These 24 nucleotides between Xho I site and SnaBI site which encodes the KEX2 and STE13 cleavage sites must be recreated in order for efficient cleavage of the fusion protein to occur. Meanwhile the stop codon (TAA) was included after the EcoR I site in reverse primer. The sequences of the primers were 5'-ATCTCGAGAAAAGAGAGGCTGAAGCTGAAGGGATCTGCAGG-3' and 5'-AATGAATTCTTAGGCTGCAACAGGGGGTAACATAAATGG-3'. A 1213 bp fragment including whole coding sequence of DC47 gene was amplified with these primers by PCR in a final volume 25 μL. Following Xho I/EcoR I digestion and purification of both vector and PCR product, the PCR product was ligated into the corresponding EcoR I and Xho I sites within the multi-cloning site (MCS) of PIRES2-EGFP plasmid. Subsequent the ligation reaction, bacterial transformation and Amp selection on LB agar plates, a few numbers of clones were obtained. A total of 10 bacterial clones were screened by PCR using the CD47-Fwd and CD47-Rev primers. Transfection of BMSCs by lipofection, and then RT-PCR for detecting CD47 gene expression after transfection.

Establishment of the myocardial fibrosis model

One-hundred healthy Sprague-Dawley, 6 weeks old (200-250 g; provided by the Experimental Animal Center of Chongqing Medical University), were used in this study. The rat were subjected to hypodermic injection with isoproterenol (batch number 080701; Shanghai Hefeng Pharmaceutical Co. Ltd, Shanghai, China) at 50 mg/kg. The injection was carried out twice a day for a continuous 10 days.

The prepared models were divided into the five groups, each containing 20 animals. The groups were: untreated, pure MSC transplanta-

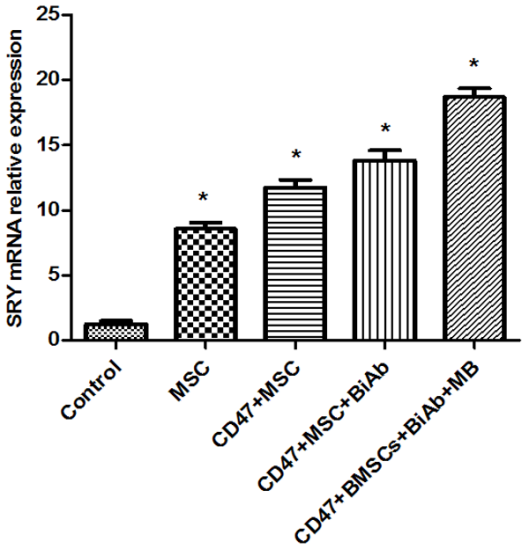

Figure 3. The mRNA expression of SRY in myocardium of the five groups of rat by qRT-PCR.

tion (MSC group); MSC with CD47 high-expression (CD47 + MSC group); MSC with CD47 high-expression combined BiAb (CD47 + MSC + BiAb group); and CD47 + MSC + BiAb + MB group. The handling of animals during these experiments was approved by the Animal Use Ethics Committee of Chongqing Medical University.

Cellular transplantation

One day after the last isoproterenol injection, all rat in each group were subjected to tail vein transfusion. The rat in the untreated group were transfused with 0.1 mL PBS., The rats were transfused with 4×10^6 MSC/kg in the MSC group and MSC CD47 + MSC group respectively. The rats in CD47 + MSC + BiAb group were transfused with 4×10^6 MSC/kg and 50 ng BiAb mixture. The rats in the CD47 + MSC + BiAb + MB group group were first transfused with 0.1 mL MB and then ultrasound wave irradiation (frequency 1 MHz, intensity 1.5 W/cm^2, duration 1 min) was performed on the precordial region. Subsequently, 4×10^6 MSC/kg and 50 ng BiAb mixture were transfused. The rats in the control group were transfused with 0.1 mL PBS.

Fluorescent quantitative polymerase chain reaction analysis on expression of the sex-determining region of Y-chromosome, vascular endothelial growth factor, matrix metalloproteinases-9, tissue inhibitor of metalloproteinase-1 in myocardium, signal transducer and activator transcription-1 and signal transducer and activator transcription-3.

Rats were killed 5 weeks after cell transplantation and their hearts collected. The cardiac apexes were sampled and subjected to fluorescent quantitative real-time polymerase chain reaction (qRT-PCR) analysis. The trizol one-step method was used to extract the total RNA and its purity was verified using an ultraviolet spectrophotometer. Reverse trancription and cDNA synthesis were carried out using conventional methods. Specific primers (**Table 1**) were designed according to the sequences of sex-determining region of Y-chromosome (SRY), matrix metalloproteinase (MMP)-9, tissue inhibitor of metalloproteinase (TIMP)-1, vascular endothelial growth factor (VEGF) and β-actin in GenBank. Primers were synthesized by Shinegene Biotechnological Co. (Shanghai, China). The TaKaRa TP (Japan) fluorescent qRT-PCR detection system was used for amplification. An SYBR green fluorescent quantitation PCR kit (Shine-gene Biotechnological Co.) was used for quantitative detection of the target genes. Each reaction system included 1 μL cDNA, 25 μL 2× SYBR Premix Ex Taq TM II buffer, 0.3 μL of each primer for the target gene (10 μM/L), and 8.4 μL RNase-free water. The expression level of β-actin was also detected as an internal control. The cycle threshold was read and the relative ration method was used for the calculation. The standard curve, amplification curves and melting curve were plotted.

Assessment of myocardial collagen with Sirius Red staining and polarized light

The transverse plane of the left ventricle with a thickness of 2 mm was collected for the preparation of successive paraffin sections to a thickness of 5 μm. This was followed by carbazotic acid-Sirius Red staining. Myocardial collagen was observed under a polarized light microscope. Image J software (version 1.43; http://rsb.info.nih.gov/ij/, 2010-01) was used for the quantitative analysis. Collagen with Sirius Red staining was analyzed using image enhancements, color processing and measuring in Image J software. Significant differences were determined by analysis of variance (ANOVA) with appropriate post-hoc testing.

Western blot analysis of signal transducer and activators of transcription 1 and 3 expression in myocardium

Fresh cardiac tissue (250-500 mg) was collected and 1 mL total protein extraction reagent containing protease inhibitor added. Total pro-

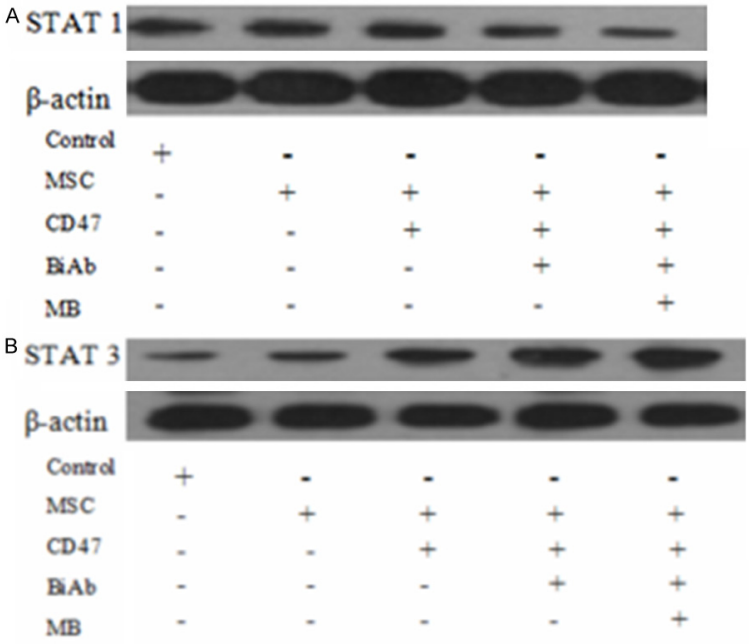

Figure 4. The protein expression of STAT 1 and STAT 3 in myocardium of the five groups of rat by WB.

teins were extracted after homogenization. Coomassie brilliant blue staining was used to determine the protein concentration. Subsequently, SDS-PAGE electrophoresis was used to separate the proteins, and proteins were transferred to a polyvinylidene fluoride (PVDF) membrane. The membrane was then incubated with rabbit anti rat signal transducer and activators of transcription (STAT)1 or STAT 3 antibodies (Aviva Systems Biology, San Diego, CA, USA.), followed with anti-rabbit IgG (Sigma, Santa Clara, CA, USA.) staining, and then subjected to film development and further analysis.

Statistical analysis

SPSS 16.0 statistical software was used for the data analysis. The measurement data were represented by mean standard deviation. An ANOVA was used to compare differences among the seven groups. A *P*-value of 0.05 was used to determine statistical significance.

Result

Identification of MSC

The in vitro cultured MSC grew in adherence and most of them grew in parallel arrays or a whirlpool-like pattern. The cells had a fusiform or polygonal shap and the karyoplasmic ratio was large (**Figure 1A**). The MSC became polygonal 1 week after osteogenic induction, and calcium content deposition between cells were observed 2 weeks after induction (**Figure 1B**). Significant formation of calcium nodes with Alizarin Red staining was observed 3 weeks after induction (**Figure 1C**). The morphology of MSC became irregular 1 week after adipogenic induction, and small fatty granules with a relatively strong refraction rate were found in the cytosol 2 weeks after nduction (**Figure 1D**). Lipid droplet accumulation with Oil Red O staining was found 3 weeks after induction (**Figure 1E**). Flow cytometry results indicated that the positive expression rates of CD29, CD44 and CD117 on MSC were 99.91%, 98.96% and 2.01%, respectively. These results indicated that the cultured cells expressed CD29 and CD44, but not CD117, which is in accordance with the phenotypic characteristics of MSC. The above-mentioned morphologic data and induced differentiation results in conjunction with the classification of cell phenotypes indicated that these cells were indeed MSC.

Identification of overexpression CD47 in MSC

After transfection, total RNA of MSC cells was detected by RT-PCR detection. It was found that, compared to empty transfection group the level of CD47 mRNA and protein expression in PIRES2-EGFP-Rat/CD47 group was significantly higher (**Figure 2**, $P<0.05$).

Homing efficiency of MSC and its functions in the treatment of myocardial fibrosis

The mRNA expression of SRY (**Figure 3**), MMP-9, TIMP-1 and VEGF in myocardium of the five groups of rat by qRT-PCR is shown in **Table 1**. Expression of SRY mRNA represented the amount of male MSC that were recruited to cardiac tissue in the receptor rat. The highest

expression of SRY was found in the CD47 + MSC + BiAb + MB group, the CD47 + MSC + BiAb group ranked second, and expression in the MSC group and CD47 + MSC were relatively low (P<0.05). Almost no expression of SRY gene was found in the control group.

Differential expression of myocardial STAT 1 and STAT 3

Five weeks after treatment administration, the expression of myocardial STAT 1 and STAT 3 was determined by Western blot. The results are shown in **Table 1**, with separate bands for STAT 1 and STAT 3. The analysis of the optical density of each band is shown in **Figure 4**.

STAT 1 expression in rat with myocardial fibrosis significantly increased compared with that of the control group (*P*<0.05). Higher levels of STAT 1 in the control was seen than in the MSC, CD47 + MSC, CD47 + MSC + BiAb, CD47 + MSC + BiAb + MB. STAT 3 expression in the MSC, MSC, CD47 + MSC, CD47 + MSC + BiAb, CD47 + MSC + BiAb + MB groups significantly increased compared with that of the control.

Discussion

We investigated the homing and therapeutic efficacy of MSC in which being CD47 over-expressed transplantation in isoproterenol-induced myocardial fibrosis mice with a combination treatment of BiAb and ultrasound-mediated MB. With the combination of BiAb and ultrasound-mediated MB, the homing number of transplanted MSC increased, MMP-9 [11] and TIMP-1 [12] decreased, and pathologic myocardial fibrosis was improved. These results may indicate a potential mechanism relevant to the STAT signaling pathway [13, 14].

BMSC transplantation is generally recognized to be the most promising stem cell therapy in treatment of ischemic heart disease due to its advantages of self-replicating ability, multi-directional differentiation potential, easily obtaining, no immune rejection, and no ethical conflicts [15-17]. However, simple BMSC transplantation has limitations because of limited survival and poor differentiation or maturation of the transplanted cells. More importantly, the adverse host micro-environment in infarction foci such as hypoxia and ischemia, ischemia-reperfusion injury with subsequent excessive inflammation in acute or subacute phase, and local structural alterations (e.g. myocardial fibrosis and micro-vascular damage) in chronic phase is not favorable to trans-planted cell surviving [18, 19]. Accordingly, it is desirable to explore a newly approach that modify not only the donor cells but the host micro-environment as well.

Prepared CD29× AMLCA is the connecting bridge between injured myocardium and MSC. AMLCA can specifically recognize injured myocardium, and CD29 is the molecular marker that shows a positive rate of more than 99% on the surface of MSC. Therefore CD29× AMLCA can bind to both MSC and injured myocardium, and it can act as the bridge between them. In the present study, we transfused MSC and BiAb in a free state into mice that suffered from isoproterenol-induced myocardial fibrosis and found that BiAb can increase the homing number of MSC, and the homing rate was even higher with the aid of ultrasound-mediated MB. These findings indicate that BiAb and ultrasound-mediated MB can guide the targeted migration of MSC [20-25]. Previous work has revealed that the transfusion of BiAb and effector cells via intravenous infusion into lymphoma mice and BiAb can assist the effector cells to bring tumor inhibiting activities into play.

Additionally, BiAb in a free state can guide effector cells to damaged tissues containing target antigen in animal models. This may be attributed to the maintenance of stronger biologic activity by MSC and BiAb, as they were not subjected to the assembly process in vitro. MMP-9 and TIMP-1 in untreated myocardial fibrosis mice were significantly upregulated and fibrous degeneration of hearts was expedited. MMP-9 and TIMP-1 levels decreased 5 weeks after MSC transplantation, but they were still higher than those of normal mice. Meanwhile, collagen deposition decreased and interstitial fibrosis was alleviated. Among the treatment groups, the homing number of MSC in the CD47 + MSC + BiAb + MB group was the highest, and the degree of myocardial fibrosis was moderate, while the expression of TIMP-1 andMMP-9 was relatively low, indicating that MSC can not only be recruited efficiently with the aid of BiAb and ultrasound-mediated MB, but can also prevent myocardial fibrosis at the homing site. These results indicated that the intervention of

MSC on myocardial fibrosis is closely related to its homing amount.

The upregulation and imbalance in MMP-TIMP expression after myocardial damage affects the degree of fibrous degeneration of heart [26-31]. Therefore, the internal mechanism for the intervention of MSC on MMP-TIMP needs to be elucidated. First, more transplanted MSC (which can ensure a greater homing amount) can regulate a pathologic MMP-TIMP imbalance, indicating that the amount of stem cells at the local target site can affect the efficacy of MMP-TIMP. Second, some investigations have found that the culture solution of MSC (not containing MSC) can regulate the expression of MMP-TIMP and inhibit the collagen secretion of cardiac fibroblasts. These results indicate that MSC can secrete many kinds of biologically active molecules, such as various growth factors, cytokines and chemical mediators (although these mechanisms remain unclear), that help MSC to function in repair at injured sites. Some investigations also indicate that MSC have anti-inflammatory functions in the target position of the transplantation, and thus exhibit anti-inflammatory mechanisms and participate in protection of the heart in ischemic heart disease.

Our investigation shows that myocardial STAT 1 expression increases in mice that suffer from myocardial fibrosis compared with normal mice. When tail vein transplantation of MSC was performed, the high expression of STAT 1 was inhibited, while the expression of STAT 3 was stimulated and upregulated. With the aid of BiAb and ultrasound-mediated MB, STAT 3 expression increased and TIMP-1 was downregulated. At the same time, the homing amount of MSC was increased, and the improvement in myocardial fibrosis was significant. These results indicate that STAT 1 is involved in myocardial fibrosis and STAT 3 is related to anti-fibrosis of MSC.

Although many investigations have indicated the superior effects of MSC on the repair of ischemic myocardium, some investigations presume that MSC transplantation is not always optimal [32, 33]. Furlani et al. found that regional injections of MSC, carried out for the treatment of rats with acute myocardial infarction, for 6 weeks did not improve heart function. These conflicting results may occur because of different treatment details and evaluation methods utilized during the early research stages in MSC transplantation therapy. In the present study, MMP-9 and TIMP-1 expression was significantly downregulated in the CD47 + MSC + BiAb + MB group, which showed the highest homing rate, and the intervention effects on myocardial fibrosis were improved; however, VEGF expression was not significantly improved. This indicates that MSC transplanted via the peripheral intravenous route can significantly improve the mesenchymal structure of the fibrotic heart to some extent, but its improvement on vascular neogenesis is not significant. Such results could be attributed to the short duration of the treatment, or intrinsic limitations of the isoproterenol-induced myocardial fibrosis model. Further treatment and investigations in long-term studies are needed.

Acknowledgements

This project was supporyed by grants from the National Nature Science Foundation of China (No. 81201101), Chongqing municipal Department of Health Foundation (No: 2012-2-057, 2015MSXM019) and Chongqing Municipal Science and Technology Foundation and cutting-edge research projects generally projects (No: cstc2015jcyjA10074). The author are thankful to all of the involved laboratories and related research members, Finally, we sincerely thank Ma ke Ph.D. student at Medical College of Qingdao University and state key laboratory of brain cognitive science in institute of biophysics, CAS for his assistance with data analysis and manuscript revision.

Disclosure of conflict of interest

None.

Address correspondence to: Dr. Qing-Wei Chen, Department of Gerontology, The No. 2 Hospital Affiliated to Chongqing Medical University, Chongqing 400010, China. Tel: 86-23-63693612; Fax: 86-23-63693612; E-mail: luoshilancq@163.com

References

[1] McNiece I. Stem cells for myocardial infarction. Cytotherapy 2015; 17: 243-244.

[2] Yu J, Wu YK, Gu Y, Fang Q, Sievers R, Ding CH, Olgin JE and Lee RJ. Immuno-modification of

enhancing stem cells targeting for myocardial repair. J Cell Mol Med 2015; 19: 1483-91.
[3] Fagan A, Asghar O, Pearce K, Stout M, Ray SG, Schmitt M and Malik RA. Medalists with extreme duration of type 1 diabetes exhibit only mild diastolic dysfunction and myocardial fibrosis. Diabetes Care 2015; 38: e5-6.
[4] Thomas TO, Jefferies JL, Lorts A, Anderson JB, Gao Z, Benson DW, Hor KN, Cripe LH and Urbina EM. Autonomic dysfunction: a driving force for myocardial fibrosis in young Duchenne muscular dystrophy patients? Pediatr Cardiol 2015; 36: 561-568.
[5] Lee SP, Lee W, Lee JM, Park EA, Kim HK, Kim YJ and Sohn DW. Assessment of diffuse myocardial fibrosis by using MR imaging in asymptomatic patients with aortic stenosis. Radiology 2015; 274: 359-369.
[6] Rodriguez-Reyna TS, Morelos-Guzman M, Hernandez-Reyes P, Montero-Duarte K, Martinez-Reyes C, Reyes-Utrera C, Vazquez-La Madrid J, Morales-Blanhir J, Nunez-Alvarez C and Cabiedes-Contreras J. Assessment of myocardial fibrosis and microvascular damage in systemic sclerosis by magnetic resonance imaging and coronary angiotomography. Rheumatology (Oxford) 2015; 54: 647-654.
[7] Bruns H, Bessell C, Varela JC, Haupt C, Fang J, Pasemann S, Mackensen A, Oelke M, Schneck JP and Schutz C. CD47 Enhances In Vivo Functionality of Artificial Antigen-Presenting Cells. Clin Cancer Res 2015; 21: 2075-2083.
[8] Xiao ZY, Banan B, Jia J, Manning PT, Hiebsch RR, Gunasekaran M, Upadhya GA, Frazier WA, Mohanakumar T, Lin Y and Chapman WC. CD47 blockade reduces ischemia/reperfusion injury and improves survival in a rat liver transplantation model. Liver Transpl 2015; 21: 468-477.
[9] Zhang H, Li F, Yang Y, Chen J and Hu X. SIRP/CD47 signaling in neurological disorders. Brain Res 2015; 1623:74-80.
[10] Soto-Pantoja DR, Kaur S and Roberts DD. CD47 signaling pathways controlling cellular differentiation and responses to stress. Crit Rev Biochem Mol Biol 2015; 1-19.
[11] Warinrak C, Wu JT, Hsu WL, Liao JW, Chang SC and Cheng FP. Expression of matrix metalloproteinases (MMP-2, MMP-9) and their inhibitors (TIMP-1, TIMP-2) in canine testis, epididymis and semen. Reprod Domest Anim 2015; 50: 48-57.
[12] Lorente L, Martin MM, Sole-Violan J, Blanquer J, Labarta L, Diaz C, Borreguero-Leon JM, Orbe J, Rodriguez JA, Jimenez A and Paramo JA. Association of sepsis-related mortality with early increase of TIMP-1/MMP-9 ratio. PLoS one 2014; 9: e94318.
[13] Stine RR, Greenspan LJ, Ramachandran KV and Matunis EL. Coordinate regulation of stem cell competition by Slit-Robo and JAK-STAT signaling in the Drosophila testis. PLoS Genet 2014; 10: e1004713.
[14] Maimon I, Popliker M and Gilboa L. Without children is required for Stat-mediated zfh1 transcription and for germline stem cell differentiation. Development 2014; 141: 2602-2610.
[15] Chen HZ, Xia R, Guo YK, Hou JL, Zhang L-z, Li ZL, Ai H, Ning G and Gao FB. [Bone mesenchymal stem cell transplantation for acute myocardial infarction: in vivo tracing with multimodality molecular imaging]. Sichuan Da Xue Xue Bao Yi Xue Ban 2014; 45: 898-902.
[16] Chen H, Guo Y and Ning G. [Advances in treatment of myocardial infarction by mesenchymal stem cell transplantation]. Sheng Wu Yi Xue Gong Cheng Xue Za Zhi 2014; 31: 939-944.
[17] Zhou Y, Wang S, Yu Z, Hoyt RF Jr, Hunt T, Kindzelski B, Shou D, Xie W, Du Y, Liu C and Horvath KA. Induced pluripotent stem cell transplantation in the treatment of porcine chronic myocardial ischemia. Ann Thorac Surg 2014; 98: 2130-2137.
[18] Li X, Zhou J, Liu Z, Chen J, Lu S, Sun H, Li J, Lin Q, Yang B, Duan C, Xing MM and Wang C. A PNIPAAm-based thermosensitive hydrogel containing SWCNTs for stem cell transplantation in myocardial repair. Biomaterials 2014; 35: 5679-5688.
[19] Yin Q, Pei Z, Wang H and Zhao Y. Cyclosporine A-nanoparticles enhance the therapeutic benefit of adipose tissue-derived stem cell transplantation in a swine myocardial infarction model. Int J Nanomedicine 2014; 9: 17-26.
[20] Rapoport N, Nam KH, Gupta R, Gao Z, Mohan P, Payne A, Todd N, Liu X, Kim T, Shea J, Scaife C, Parker DL, Jeong EK and Kennedy AM. Ultrasound-mediated tumor imaging and nanotherapy using drug loaded, block copolymer stabilized perfluorocarbon nanoemulsions. J Control Release 2011; 153: 4-15.
[21] Evjen TJ, Nilssen EA, Barnert S, Schubert R, Brandl M and Fossheim SL. Ultrasound-mediated destabilization and drug release from liposomes comprising dioleoylphosphatidylethanolamine. Eur J Pharm Sci 2011; 42: 380-386.
[22] Polat BE, Hart D, Langer R and Blankschtein D. Ultrasound-mediated transdermal drug delivery: mechanisms, scope, and emerging trends. J Control Release 2011; 152: 330-348.
[23] Wang S, Raju BI, Leyvi E, Weinstein DA and Seip R. Acoustic accessibility investigation for ultrasound mediated treatment of glycogen storage disease type Ia patients. Ultrasound Med Biol 2011; 37: 1469-1477.
[24] Wang CY, Yang CH, Lin YS, Chen CH and Huang KS. Anti-inflammatory effect with high intensity focused ultrasound-mediated pulsatile deliv-

ery of diclofenac. Biomaterials 2012; 33: 1547-1553.
[25] Deng W, Chen QW, Li XS, Liu H, Niu SQ, Zhou Y, Li GQ, Ke DZ and Mo XG. Bone marrow mesenchymal stromal cells with support of bispecific antibody and ultrasound-mediated microbubbles prevent myocardial fibrosis via the signal transducer and activators of transcription signaling pathway. Cytotherapy 2011; 13: 431-440.
[26] Horio T and Kawano Y. [MMP/TIMP ratio and hypertensive target organ damage]. Nihon Rinsho 2006; 64 Suppl 6: 171-175.
[27] Wu YG and Wang LX. [Function of MMP/TIMP on airway remodeling of bronchial asthma and treating effects of Zhichuan capsule]. Zhong Xi Yi Jie He Xue Bao 2004; 2: 435-439.
[28] Stratmann B, Farr M and Tschesche H. MMP-TIMP interaction depends on residue 2 in TIMP-4. FEBS Lett 2001; 507: 285-287.
[29] Maatta M, Soini Y, Liakka A and Autio-Harmainen H. Localization of MT1-MMP, TIMP-1, TIMP-2, and TIMP-3 messenger RNA in normal, hyperplastic, and neoplastic endometrium. Enhanced expression by endometrial adenocarcinomas is associated with low differentiation. Am J Clin Pathol 2000; 114: 402-411.
[30] Li H, Simon H, Bocan TM and Peterson JT. MMP/TIMP expression in spontaneously hypertensive heart failure rats: the effect of ACE- and MMP-inhibition. Cardiovasc Res 2000; 46: 298-306.
[31] Fortunato SJ, Menon R and Lombardi SJ. MMP/TIMP imbalance in amniotic fluid during PROM: an indirect support for endogenous pathway to membrane rupture. J Perinat Med 1999; 27: 362-368.
[32] Tsai CY, Chua S, Leu S, Chang AY, Chan JY and Chan SH. VEGF tonically sustains myocardial performance via fetal liver kinase-1 in the heart. Int J Cardiol 2014; 177: 727-730.
[33] Moon HH, Joo MK, Mok H, Lee M, Hwang KC, Kim SW, Jeong JH, Choi D and Kim SH. MSC-based VEGF gene therapy in rat myocardial infarction model using facial amphipathic bile acid-conjugated polyethyleneimine. Biomaterials 2014; 35: 1744-1754.